Aerosol optical properties and radiative forcing over mega-city Karachi

Khan Alam [a,c,*], Thomas Trautmann [b], Thomas Blaschke [a,c]

[a] *Department of Geography and Geology, University of Salzburg, Hellbrunnerstrasse 34, Salzburg 5020, Austria*
[b] *German Aerospace Centrer, Remote Sensing Technology Institute, Oberpfaffenhofen, 82234 Wessling, Germany*
[c] *Z_GIS, Centre for Geoinformatics, University of Salzburg, Hellbrunnerstrasse 34, Salzburg 5020, Austria*

ARTICLE INFO

ABSTRACT

Aerosol optical properties have been analyzed through the ground-based Aerosol Robotic Network (AERONET) over the mega city Karachi during August 2006–July 2007. The aerosol optical depth (AOD) is strongly dependent on wavelength; for shorter wavelengths AOD values are higher than at longer wavelengths. The results reveal that the monthly average AOD at 500 nm ranges from 0.31 to 0.92 with an annual mean of 0.48 ± 0.18 and monthly averaged angstrom exponent (Alpha) ranges from 0.17 to 1.05 with an annual mean of 0.49 ± 0.31. The maximum monthly average AOD value of 0.92 ± 0.28 with the corresponding Alpha value of 0.21 ± 0.11 is found for July 2007, while the minimum monthly average AOD value of 0.31 ± 0.11 with the corresponding Alpha value of 0.53 ± 0.13 is recorded for March 2007. The volume size distribution in the coarse mode is higher in summer and lower in winter, whereas in the accumulation mode the volume size distribution is higher in winter than in other seasons due to the hygroscopic growth of aerosol particles. The single scattering albedo (SSA) during spring, autumn and summer seasons shows a slight increase with the wavelength and ranges from 0.88 ± 0.02 to 0.97 ± 0.01. The asymmetry parameter (ASY) is also wavelength dependent and varies from 0.61 ± 0.03 to 0.74 ± 0.02 during the year. The aerosol radiative forcing (ARF) for the whole observation period at the top of the atmosphere (TOA) is in the range of -7 to -35 Wm^{-2} (average -22 ± 6 Wm^{-2}), at the surface from -56 to -96 Wm^{-2} (average -73 ± 12 Wm^{-2}), increasing the atmospheric forcing from $+38$ to $+61$ Wm^{-2} (average $+51 \pm 13$ Wm^{-2}). The SBDART-AERONET radiative forcing at the surface and TOA agree with correlation of 0.92 and 0.82, respectively.

1. Introduction

Aerosol radiative forcing (ARF) is intended to be a useful way to compare different causes of perturbations in the climate system. In the last two decades, aerosols have been recognized as a major factor in determining global climate change (Intergovernmental Panel on Climate Change, IPCC, 2007) since they play a crucial role in the solar and thermal radiative transfer in the atmosphere (Kosmopoulos et al., 2008). The ARF is generally classified as direct forcing and involves scattering and absorption of solar radiations by aerosols in a cloud free sky and indirect forcing through their fundamental role in cloud microphysics. The various aerosol types have different effects on the sign and magnitude of the ARF (Kaskaoustis et al., 2007). For example, black carbon (BC) aerosols have considerably contributed to global warming (Jacobson, 2001; Penner et al., 2003), and appear to be responsible to increase rainfall in the southern part of China and drought in the northern parts of China (Menon et al., 2002, Sarkar et al., 2006). Smoke particles from biomass burning may have a significant impact on climate particularly in altering the global radiation balance (Badarinath et al., 2009; Kumar et al., 2010). Dust particles modify the transport of the shortwave as well as long-wave radiation through the atmosphere by scattering and absorption processes (Otto et al., 2007), and thus heating the atmospheric column due to dust absorption (Haywood et al., 2001). Several other studies have been conducted on the optical properties of

* Corresponding author at: Department of Geography and Geology, University of Salzburg, Hellbrunnerstrasse 34, Salzburg 5020, Austria. Tel.: +43 681 10787864.
E-mail address: khanalamso@gmail.com (K. Alam).

mineral dust aerosols, their seasonal, spatial and temporal characteristics, and their influence on solar radiation budget (Ge et al., 2010; Jayaraman, et al., 2006; Liu et al., 2008; Prasad et al., 2007; Ramanathan et al., 2001; Singh et al., 2010; Smirnov et al., 2001; Tegen et al., 2004; Zheng et al., 2008).

Aerosol radiative forcing and optical properties have not been studied in the Karachi region. This region is one of the 'hotspots' of atmospheric brown clouds (ABCs) in Asia with annual mean AOD values greater than 0.3 and the absorption optical depth being 10% of the AOD. ABCs are basically layers of air pollution consisting of aerosols such as BC, organic carbon, dust, sulfates, nitrates, and fly ash (Ramanathan et al., 2005). The annual mean surface dimming and atmospheric solar heating by ABCs over Karachi, Beijing, Shanghai and New Delhi are found to be in the range from 10 to 25% (Ramanathan et al., 2008). Some studies have been conducted in Karachi to monitor the aerosol concentrations in terms of total suspended particulate loading (Parekh et al., 2001) and black carbon concentration (Dutkiewicz et al., 2009). Recently, Alam et al. (2010) have analyzed the spatio-temporal variation of aerosol optical depth (AOD) and the aerosol influence on cloud parameters using Moderate Resolution Imaging Spectroradiometer (MODIS) data. In the present study we used Aerosol Robotic Network (AERONET) data for the first time to analyze the aerosol optical properties with the aim to investigate the monthly spectral variations in AOD and Angstrom exponent (Alpha) over Karachi. The study also analyzes the seasonal variability of aerosol in terms of the size distribution, and investigates the variability of single scattering albedo (SSA), asymmetry parameter (ASY) as well as real and imaginary parts of the refractive index (RI). This study also carries out the computations of ARF using the Santa Barbara DISORT Atmospheric Radiative Transfer (SBDART) model (Ricchiazzi et al., 1998). This paper consists of four sections. Section 1 describes the introduction to the paper. Section 2 describes experimental site and instrumentation, Section 2.4 provides aerosol optical properties (AOD, Alpha, size distribution, SSA, ASY, and RI) and ARF calculations. Conclusions are given in Section 3.

2. AERONET sampling site and Instrumentation

2.1. Site description

Karachi is located in the southeastern part of Pakistan (Lat 24º 51′N; Long 67º 02′E) on the Arabian Sea. It is the largest city of the country with a population of more than 16 millions and covers an area of around 3500 km^2. The city has 1.5 million registered vehicles; therefore vehicular traffic is one of the main sources of atmospheric aerosol. Its climate is relatively mild, subtropical/arid with scanty rainfall (mean annual rainfall 170 mm with maximum occurs through July–September). Karachi has a large industrial base and the major industries include textiles, pharmaceutical, cement factories, oil refineries, automobiles, chemicals, heavy machinery, shipbuilding and a steel mill. Some of the main industrial zones and major roads are shown in the map (Fig. 1). The AERONET site (sampling site) is the north-west of Karachi Airport adjacent to the University of Karachi campus. The sunphotometer is located on the roof top of a 3 story building at a height of 12 m above ground level.

2.2. Instrument

The ground-based CIMEL sky radiometer (Karachi AERONET station) is operational since August 2006 under the joint collaboration between NASA and the Institute of Space Technology Karachi office. AERONET data are available at three levels; level 1.0 (unscreened), level 1.5 (cloud screened) (Smirnov et al., 2000) and level 2.0 (quality assured) (Holben et al., 1998) and can be downloaded from the AERONET website (http://aeronet.gsfc.nasa.gov/).

The CIMEL sun/sky radiometer takes measurements of the direct sun and diffuse sky radiances within the spectral ranges of 340–1020 nm and 440–1020 nm, respectively (Holben et al., 1998). The inversion algorithm (Dubovik et al., 2000) provides improved aerosol retrievals by fitting the entire measured field of radiances-sun radiance and angular distribution of sky radiances at four wavelengths (440, 670, 870, and 1020 nm) to the radiative transfer model (Dubovik et al., 2002). The inversion algorithm is used for retrieving aerosol volume size distributions in the size range from 0.05 to 15 μm together with spectrally dependent complex RI, SSA and ASY parameters from spectral sun and sky radiance data. The uncertainty of the retrieval of AOD under cloud free condition is <±0.01 for λ>440 nm and <±0.02 for shorter wavelengths, which is less than ±5 for the retrieval of sky radiance measurements (Dubovik et al., 2000). Retrieval errors in dV(r)/dlnr typically do not exceed 15–35% (depending on the aerosol type) for each particle radius bin within the 0.1–7 μm range. The errors for very small particles (0.05–0.1 μm) and very large particles (7–15 μm) may be as large as 35–100% for a given particle radius bin. Single scattering albedos are expected to have an uncertainty of 0.03–0.05 depending on aerosol type and loading (Dubovik et al., 2000). The comprehensive explanation of sun/sky radiometer retrievals accuracy along with the inversion algorithm is discussed by Dubovik et al. (2000) and Smirnov et al. (2001). In the present study, level 2.0 data were used both for direct sun (AOD and Alpha) and for inversion products for the time period of August 2006 to July 2007. Level 2.0 inversion product for March 2007 has not been released. The period (August 2006–July 2007) is rather typical in terms of dust loadings, therefore the study of aerosol optical properties in this region is of great importance. We used AOD at five wavelengths (440, 500, 675, 870 and 1020 nm) along with Alpha (440–870), SSA, ASY parameters and complex RI at four wavelengths (440, 675, 870, and 1020 nm). We have also used a dust image from the MODIS Terra satellite for July 21, 2007.

2.3. Meteorological conditions

The average prevailing meteorological conditions during the study period are shown in Fig. 2. Data for monthly mean wind speeds, wind direction, maximum and minimum temperature and relative humidity and total precipitation are obtained from Pakistan Meteorological Department. The mean maximum and minimum temperatures are in the range from 26.3–36 °C and 13–29 °C, respectively. The mean ambient relative humidity varies in the range from 31 to 76%. The mean wind speed ranged from 2.05 to 5.40 m/s with lower value in November 2006 and maximum in June 2007. During the study period the winds are predominantly directed almost from southwest. The Karachi area receives very little rainfall:

Fig. 1. Map of Karachi showing the sampling site, major roads and industries.

the total annual rainfall for the study period is 432.7 mm with a monthly maximum of 148.6 mm occurring in August 2006.

2.4. Aerosol optical depth and angstrom exponent

The AOD is retrieved at five wavelengths 440, 500, 675, 870 and 1020 nm from the AERONET direct sun product. The spectral variations of monthly mean AOD from August 2006 to July 2007 are shown in Fig. 3a. The monthly means are calculated on the basis of daily mean AOD, which are in the range of 0.12–1.01. It is evident from Fig. 3a that the AODs are strongly dependent on wavelength: for longer wavelengths AOD values are lower than for shorter wavelengths.

The AOD values for July 2007 are the highest for the period investigated at all wavelengths. Singh et al. (2004) reported spectral variation in AOD and also found the highest values for the month of July, for both 2003 and 2004. During this period mostly dust activities occur in the south of Pakistan on the coast of the Arabian Sea.

Fig. 3b shows the monthly variations of AOD at 500 nm from August 2006 to July 2007, with the error bars showing the standard deviation of the monthly averaged value along with Alpha (400–870 nm). Alpha is determined from the spectral dependence of the measured optical depth, and is a good indicator for the aerosol size. High values of alpha indicate the dominance of fine particles, whereas low values indicate the dominance of coarse particles and relatively less concentration of fine particles. Alpha values are in the range 0.17–1.05, with the lowest value in June and highest value in December. Both AOD and Alpha vary inversely to each other. The annual average AOD at 500 nm is found to be 0.48 ± 0.18 with an annual average Alpha 0.49 ± 0.31 during the period of observations. The monthly average AOD shows a maximum value of 0.92 ± 0.28 for July 2007 with the corresponding Alpha value of 0.21 ± 0.11 (Table 1). This means that aerosol
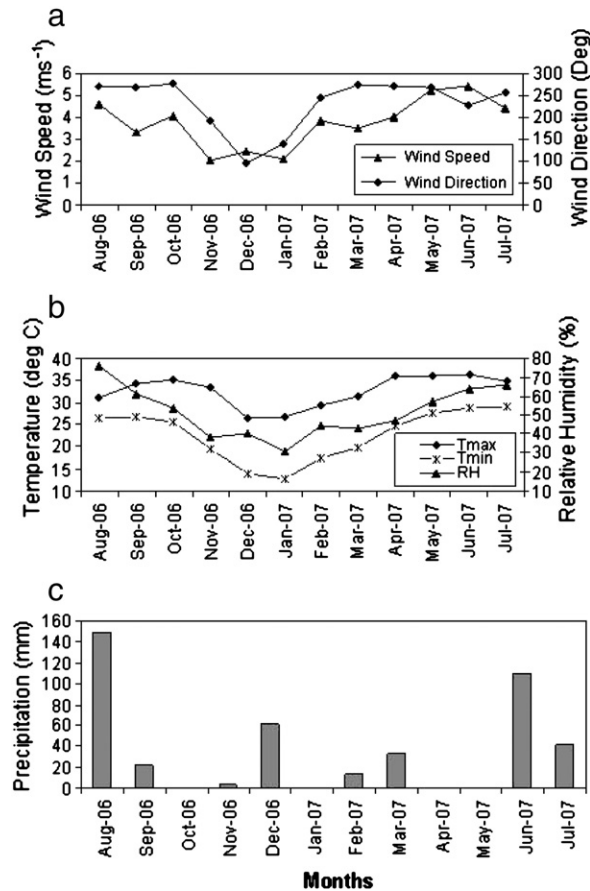
Fig. 2. Prevailing meteorological conditions for the study area during August 2006 to July 2007.

particles are larger during this period and are likely related to dust activities. Behnert et al. (2007) found that sea salt and Saharan dust are associated with low α values representing the large size of the particles.

The Moderate Resolution Imaging Spectroradiometer (MODIS) Terra satellite captured dust plumes through Afghanistan and Pakistan on July 21, 2007 (NASA Earth Observatory Natural Hazards, 2007) as shown in Fig. 4. The dust appeared as a beige swirl over the arid landscape. The pale color of this dust plume was consistent with that of dried wetland soils. A break in the plume allowed a relatively clear view of the land surface along the border between southern Afghanistan and Pakistan. The dust storm originated from the Hamoun wetland. On the same day (21st July) AOD and Alpha values were observed to be 1.36 and 0.06 respectively. Alam et al. (2010) reported a very high AOD value of 0.80 ± 0.34 in Karachi during summer, which can be attributed to the fact that it is a large urban, industrial area but at the same time a coastal city.

In November 2006, AOD and Alpha are found to be 0.52 ± 0.28 and 0.77 ± 0.20, which indicate that there is an increase in the contribution of fine particles during this high temperature period (Liu et al., 2008; Zheng et al., 2008). The local and/or regional pollutants along with atmospheric convection might play a major role in the increase in AOD. Dutkiewicz et al.
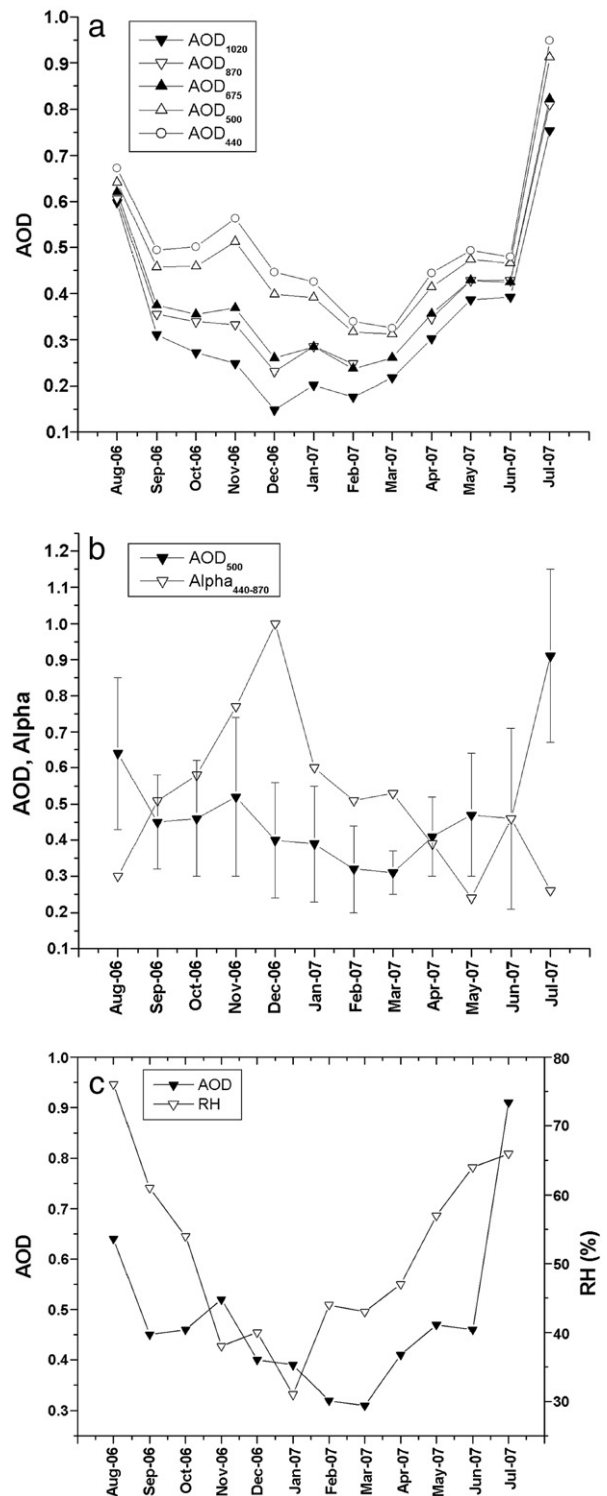

Fig. 3. Monthly average variations in (a) AOD at different wavelengths (b) AOD at 500 nm and Alpha (440–870) and c AOD and RH during August 2006 to July 2007.

(2009) reported that high black carbon concentrations ($15\ \mu gm^{-3}$) also contribute to high AOD values during November, 2006 in Karachi. The AOD starts increasing from

Table 1
Mean AOD at a wavelength of 500 nm and Alpha (440–870) from August 2006 to July 2007.

Months	Mean AOD (500 nm) ± SD	Mean Alpha (440–870) ± SD
Aug 2006	0.65 ± 0.12	0.30 ± 0.03
Sep 2006	0.45 ± 0.14	0.51 ± 0.16
Oct 2006	0.46 ± 0.15	0.58 ± 0.27
Nov 2006	0.52 ± 0.28	0.77 ± 0.20
Dec 2006	0.40 ± 0.14	1.01 ± 0.26
Jan 2007	0.39 ± 0.12	0.61 ± 0.26
Feb 2007	0.40 ± 0.08	0.54 ± 0.15
Mar 2007	0.31 ± 0.11	0.53 ± 0.13
Apr 2007	0.41 ± 0.12	0.39 ± 0.20
May 2007	0.47 ± 0.14	0.24 ± 0.11
Jun 2007	0.46 ± 0.24	0.19 ± 0.09
Jul 2007	0.92 ± 0.28	0.21 ± 0.11

the month of May 2007 and reaches the peak value in July 2007. The AOD during December 2006 and January 2007 is comparatively higher than the AOD during February and March, 2007 as shown in Table 1. On the other hand the Alpha values for December 2006 and January 2007 are high, indicating the presence of fine particles in the atmosphere.

Fig. 3c shows that AOD has a nearly similar monthly variation as that of RH. Both AOD and RH are higher in July and August than for all other months. The increase in RH leads to particle growth, to an increase of scattering, and to an associated increase in AOD, SSA and asymmetry parameters. Water vapor and AOD are directly related to each other, and hence a higher concentration of water vapor in summer leads to a higher AOD (Alam et al., 2010; Ranjan et al., 2007). The

water uptake of atmospheric aerosols is important as it can have a number of consequences: it can alter both the size and the chemical composition of particles, and consequently their optical properties (Alam et al., 2010). Changes in aerosol water uptake behavior can therefore, at least potentially, lead to changes in both direct and indirect radiative forcing on climate (Intergovernmental Panel on Climate Change, IPCC, 2001, Intergovernmental Panel on Climate Change, IPCC, 2007).

2.5. Seasonal variation in aerosol size distribution

The size distribution of aerosols is an important parameter in understanding their effect on climate. The worldwide aerosol size distribution exhibits two distinct modes: fine particles with particle size <0.6 μm and coarse with particle size >0.6 μm (Dubovik et al., 2002). The AERONET aerosol size distributions are retrieved from the Sun photometer using 22 radius size bins in the size range of 0.05–15 μm. The seasonal variations in aerosol volume size distributions for the period of August 2006 to July 2007 are shown in Fig. 5. The volume size distributions exhibit a bimodal structure, which can be characterized by the sum of two log-normal distributions as follows:

$$\frac{dV(r)}{d\ln r} = \sum_{i=1}^{2} \frac{C_{V,i}}{\sqrt{2\pi}\sigma_i} \exp\left[-\frac{\left(\ln r - \ln r_{V,i}\right)}{2\sigma_i^2}\right]$$

Where r_V is the volume median radius, C_V is the volume concentrations and σ is the geometric standard deviation.
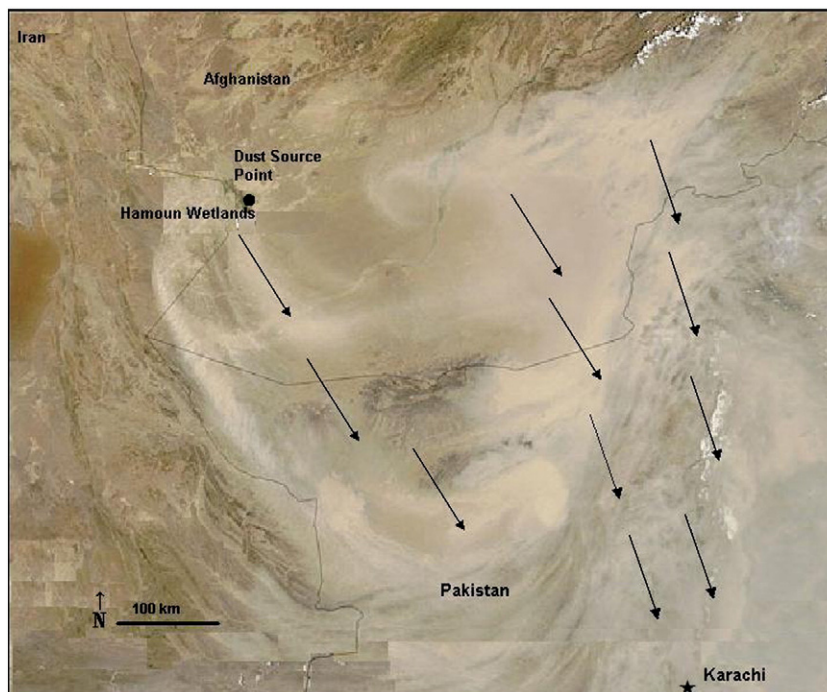

Fig. 4. Dust plumes originated from Hamoun Wetlands in the southern part of Pakistan and Afghanistan on 21st July, 2007. On this day AERONET AOD and Alpha values were observed to be 1.38 and 0.07, respectively. The arrows show the direction of plumes towards Karachi.
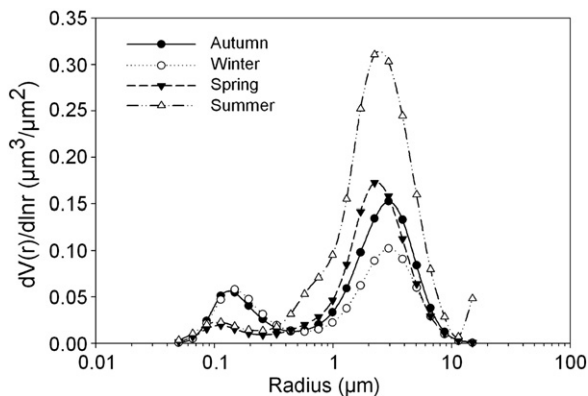
Fig. 5. Seasonal variations in AERONET retrieved aerosol size distributions during August 2006 to July 2007.

These quantities are calculated using the following expressions:

$$\ln r_V = \frac{\int\limits_{r_{min}}^{r_{max}} \ln r \frac{dV(r)}{d\ln r} d\ln r}{\int\limits_{r_{min}}^{r_{max}} \frac{dV(r)}{d\ln r} d\ln r}$$

$$\sigma_V = \sqrt{\frac{\int\limits_{r_{min}}^{r_{max}} (\ln r - \ln r_V)^2 \frac{dV(r)}{d\ln r} d\ln r}{\int\limits_{r_{min}}^{r_{max}} \frac{dV(r)}{d\ln r} d\ln r}}$$

$$C_V = \int\limits_{r_{min}}^{r_{max}} \frac{dV(r)}{d\ln r} d\ln r$$

where r_{min} and r_{max} denote the radius ranges for corresponding modes. It is evident from Fig. 5 that the size distribution in the accumulation mode is dominant at about 0.15 μm, whereas the coarse mode is dominant with a radius of about 3 μm. The volume size distributions in the coarse mode are higher in summer and lower in the winter season; the higher values in summer are due to the dust activities during this season and also due to meteorological conditions, such as temperature, pressure, and relative humidity. Alam et al. (2010) found that

hygroscopic aerosols increased the AOD over the southern coastal areas of Pakistan during the humid summer season. The AOD is found to be in the range of 0.25 to 1.38 during the summer season. During the summer season, aerosol size distribution shows 40–70% increase in the volume concentration in the coarse mode as compared to other seasons. Tripathi et al. (2005) also found 50% increase in volume concentration in the coarse mode as compared to the yearly average aerosol size distribution during pre-monsoon and monsoon seasons. The volume concentration in the accumulation mode is highest in the winter season. The increase in volume concentration in the accumulation mode during the winter season is due to the hygroscopic growth of the ambient particles (Singh et al., 2004; Tripathi et al., 2005). High fluctuations in aerosol volume size distributions over Karachi occur in the coarse mode, whereas minor fluctuations are observed for the fine aerosol mode. Similar variations in aerosol volume size distribution in the coarse mode are found in Bahrain using AERONET measurements (Smirnov et al., 2001). The errors for the particle retrieval in the size range $(0.1 \leq r \leq 7\,\mu m)$ do not exceed 10% in the maxima of the size distribution and may increase up to about 35% for the points corresponding to the minimum values of $dV(r)/d\ln r$ in this size range (Dubovik et al., 2002). However, for the sizes less than 0.1 μm and higher than 7 μm the accuracy of the size distribution retrieval drops significantly, because of the low sensitivity of the aerosol scattering at 0.44, 0.67, 0.87 and 1.02 μm to particles of these sizes. It is known that the aerosol particle size distributions $dV(r)/d\ln r$ have typically low values at the edges of the respective retrieval size interval and that the relatively high errors do not significantly affect the derivation of the main features of the aerosol particle size distribution (Dubovik et al., 2000, 2002).

2.6. Single scattering albedo, asymmetry parameter

The Single scattering albedo (SSA) and asymmetry parameter (ASY) provide useful information about scattering and absorption of aerosols and are very important components in climate model radiative transfer calculations. The SSA is the ratio of scattering efficiency to total extinction efficiency, whereas ASY is the cosine-weighted average of the scattering angle for the scattered radiation. Monthly averaged SSA and ASY values and corresponding standard deviations at 440, 675, 870 and 1020 nm are shown in Table 2. SSA is found to be wavelength dependent due to the influence of dust activities

Table 2
Monthly averaged SSA and ASY with corresponding standard deviations during August 2006 to July 2007.

Month	Single-scattering albedo				Asymmetry parameter			
	440 nm	675 nm	870 nm	1020 nm	440 nm	675 nm	870 nm	1020 nm
Aug 2006	0.92 ± 0.03	0.94 ± 0.02	0.94 ± 0.01	0.95 ± 0.01	0.71 ± 0.02	0.70 ± 0.02	0.69 ± 0.02	0.69 ± 0.02
Sep 2006	0.92 ± 0.03	0.93 ± 0.03	0.94 ± 0.03	0.95 ± 0.03	0.73 ± 0.02	0.70 ± 0.02	0.68 ± 0.02	0.69 ± 0.02
Oct 2006	0.93 ± 0.02	0.93 ± 0.02	0.93 ± 0.02	0.93 ± 0.02	0.72 ± 0.02	0.68 ± 0.02	0.66 ± 0.03	0.67 ± 0.03
Nov 2006	0.92 ± 0.02	0.92 ± 0.02	0.91 ± 0.02	0.91 ± 0.02	0.72 ± 0.01	0.65 ± 0.02	0.61 ± 0.03	0.61 ± 0.03
Dec 2006	0.92 ± 0.02	0.90 ± 0.02	0.89 ± 0.03	0.88 ± 0.03	0.74 ± 0.02	0.66 ± 0.02	0.61 ± 0.04	0.60 ± 0.04
Jan 2007	0.91 ± 0.03	0.90 ± 0.03	0.90 ± 0.03	0.89 ± 0.03	0.72 ± 0.02	0.67 ± 0.02	0.64 ± 0.04	0.64 ± 0.04
Feb 2007	0.90 ± 0.01	0.90 ± 0.01	0.91 ± 0.01	0.91 ± 0.01	0.73 ± 0.02	0.70 ± 0.01	0.69 ± 0.02	0.69 ± 0.01
Apr 2007	0.88 ± 0.02	0.92 ± 0.02	0.93 ± 0.02	0.94 ± 0.01	0.73 ± 0.02	0.70 ± 0.02	0.69 ± 0.02	0.70 ± 0.02
May 2007	0.91 ± 0.02	0.95 ± 0.02	0.96 ± 0.02	0.97 ± 0.01	0.74 ± 0.02	0.72 ± 0.01	0.71 ± 0.01	0.71 ± 0.01
Jun 2007	0.91 ± 0.02	0.94 ± 0.03	0.95 ± 0.03	0.96 ± 0.03	0.74 ± 0.01	0.73 ± 0.01	0.72 ± 0.01	0.73 ± 0.01
Jul 2007	0.93 ± 0.01	0.95 ± 0.01	0.96 ± 0.01	0.97 ± 0.01	0.74 ± 0.01	0.73 ± 0.01	0.72 ± 0.01	0.72 ± 0.01

during spring, autumn and summer seasons. SSA shows a slight increasing trend with wavelength (Cheng et al., 2006b; Dubovik et al., 2002; Xia et al., 2005). The SSA at 440 nm and 675 nm varies from 0.88 ± 0.02 (in April) to 0.93 ± 0.01 (in July) and from 0.90 ± 0.01 (Dec, Jan, Feb) to 0.95 ± 0.01 (in July), respectively. Likewise, the SSA at 870 nm and 1020 nm ranges from 0.89 ± 0.03 (in Dec) to 0.96 ± 0.01 (in July) and 0.88 ± 0.03 (Dec) to 0.97 ± 0.01 (July), respectively. Overall, the SSA values are lower in winter and higher in summer. The maximum SSAs are found in summer and are 0.920, 0.947, 0.954, and 0.962 at 440, 675, 870 and 1020 nm, respectively. This is slightly lower than the SSA values reported by others for desert dust (0.95–0.99) (Dubovik et al., 2002; Kaufman et al., 2001), which suggest the possible combination of dust, urban industrial particles and sea salt aerosols over the Karachi region.

Fig. 6 shows the monthly mean spectral variation of SSA over the period August 2006 to July 2007. During summer (June, July, August) when the dust aerosols are dominant over the local pollutions and the atmosphere has more water soluble particles, SSA significantly increases with increasing wavelength. SSA also increases related to wavelength in April and May, as the high temperature during this period plays a vital role in heating and lifting loose material from soil due to higher wind speeds. Singh et al. (2004) found that during pre-monsoon and monsoon seasons water soluble aerosols grow hygroscopically in the presence of water vapor and contribute to higher SSA values at higher wavelengths. During the months October and November the SSA variation is nearly flat and there is the possibility of mixed aerosols (dust and anthropogenic aerosols). Contrarily, during winter (December–January) the absorbing urban aerosols are dominant over Karachi consequently leading to SSA decreases with increasing wavelengths, which is attributed to the presence of a mixture of aerosols from multiple sources. Similar decrease in SSA with wavelength is reported by Zheng et al. (2008). Singh et al. (2004) also reported that the SAA is strongly wavelength dependent during the winter season and varies in the range of 0.75 to 0.98 throughout the year. The ASY parameter values vary from 0.74 ± 0.02 to 0.71 ± 0.02, 0.73 ± 0.01 to 0.65 ± 0.02, 0.72 ± 0.01 to 0.61 ± 0.03, and 0.73 ± 0.01 to 0.60 ± 0.04 at 440, 675, 870 and 1020 nm, respectively. The ASY parameter

decreases with wavelength and the overall range varies from 0.74 to 0.60 for the four wavelengths.

2.7. Refractive index

The real and imaginary parts of the refractive index (RI) provide indication of high scattering or highly absorbing type of aerosols. The useful information about the RI comes from aureole radiances, which are strongly affected by errors in the angle-pointing bias. The errors are estimated 30–50% for the imaginary part and ± 0.04 for the real part of the RI (Dubovik et al., 2002). These estimated errors are for high aerosol loading ($\tau_{aero}(440) \geq 0.5$) at solar zenith angle $> 50°$. Fig. 7a shows the monthly averaged real parts of the RI at 440, 675, 870 and 1020 nm. The real part of RI at higher wavelengths is larger than at shorter wavelengths due to the higher absorption in the near infrared band by coarse particles (Cheng et al., 2006a, 2006b). The real parts of RI are found in

Fig. 7. Spectral variations of the (a) real parts and (b) imaginary parts of the refractive index during August 2006 to July 2007.
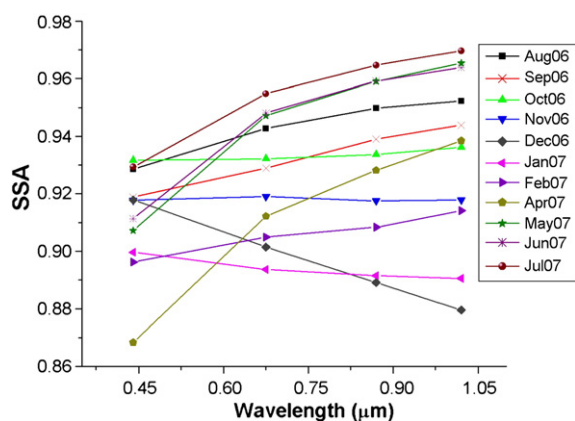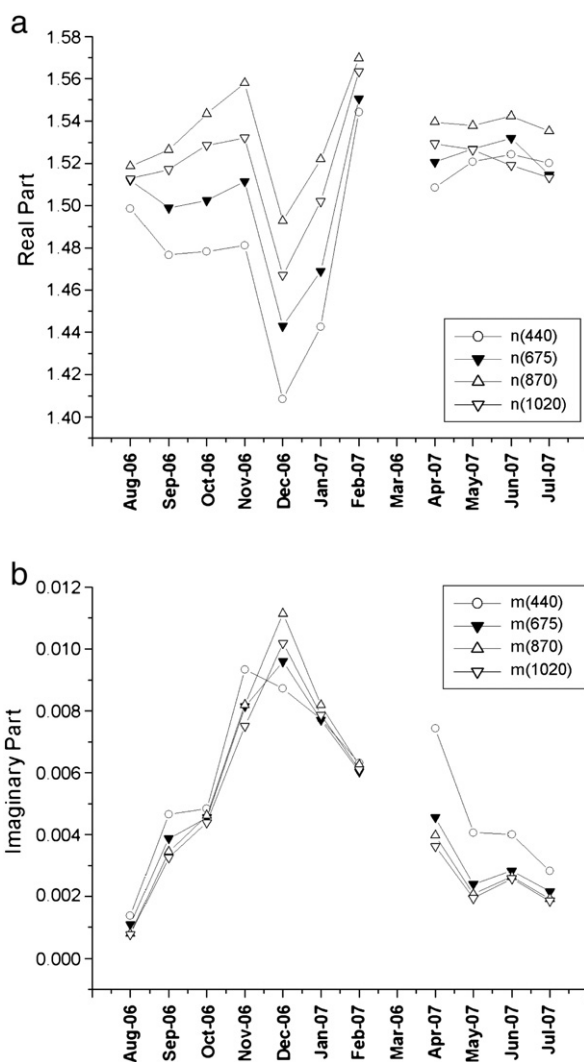
Fig. 6. Monthly average spectral variation of single scattering albedo (SSA) over Karachi during August 2006 to July 2007.

the range of 1.41 to 1.57. The real part of RI at 870 nm is higher than at 1020 nm. The highest RI for the real part is 1.57 (870 nm) in February 2007, where as the lowest is 1.41 (440 nm) in December. The lowest value in December is due to the anthropogenic activities, whereas the highest value in February is inconsistent with observed AOD and size distribution. The real parts of RI are also high (1.56 at 870 nm) in November 2006 due to some dust events in the south of Pakistan on the coast of the Arabian Sea (Alam et al., 2010). The values of the real part for August 2006 and April to July 2007 showed moderate wavelength dependency, which is probably associated with high relative humidity and also could be due to complex mineralogy during long range transportation.

The real part of RI of dust aerosols is greater than that of anthropogenic aerosols (Liu et al., 2008). In the present study we found high real part (1.57) for February, which is not the typical dust loading period, while in summer (May–July) (dust loading period) the real part ranges from 1.52 to 1.54 which is comparable to the results reported by Prasad et al. (2007) and Tripathi et al. (2005).

Fig. 7b shows the spectral variations in the imaginary parts of the RI. The imaginary part is also wavelength dependent and generally decreases as the wavelength increases, but in winter (December and January) the imaginary parts increase as wavelength increases. The imaginary part is highest during December, which shows that anthropogenic aerosols are dominant during this period. The higher imaginary part values at the two shortest wavelengths (440 nm and 670 nm) are attributed to the absorption of organic carbon/black carbon (Arola et al., 2011). On the contrary, the imaginary parts values are lower in summer (May–August). This suggests that dust aerosols are dominant during the summer season. Similar to the conditions found over India (Singh et al., 2004).

2.8. Aerosol radiative forcing

The aerosol radiation forcing (ARF) at the top of the atmosphere (TOA) or at the surface is defined as the difference in the net solar fluxes (down minus up) (solar plus long wave; in Wm^{-2}) with and without aerosol. The difference of the two gives the ARF in the whole atmosphere. In the present case the net flux was computed in the wavelength range 0.3–4.0 μm with and without aerosols at the TOA and at the surface separately using the SBDART model (Ricchiazzi et al., 1998). This model has been developed by the atmospheric science community and is being used widely for the radiative transfer calculations. In the present study the model is run at 1 h intervals for a 24 h period, and the integrated average forcing is estimated during clear sky days for every month in the period from August 2006 to July 2007. The parameters crucial for ARF estimations are AOD, SSA, ASY and surface albedo. Other input parameters in the model include solar zenith angle, which is calculated using one small code in the SBDART by specifying a particular date, time, latitude and longitude, and atmospheric profiles (humidity, temperature, ozone and other gasses). Based on the prevailing weather conditions and measured parameters, we used the mid-latitude summer atmospheric model. The AOD, SSA, and ASY have been taken from the Karachi AERONET site and were used for the ARF calculations. The surface albedo values are obtained from the Aura OMI version 3 reflectivity data through the Giovanni online data

system, developed and maintained by the NASA GES DISC (http://disc.sci.gsfc.nasa.gov/giovanni). The monthly average ARF variations at TOA, at the surface and in the atmosphere during the period August 2006 to July 2007 are shown in Fig. 8. The ARF at TOA, surface and in the atmosphere are found to be in the range of -7 to $-35\,Wm^{-2}$, -56 to $-96\,Wm^{-2}$ and $+38$ to $+61\,Wm^{-2}$, respectively. For northwestern China, Ge et al. (2010) found the surface forcing ranging from -7.9 to $-35.8\,Wm^{-2}$, which are lower values than our results. The averaged forcing for the whole period of observations at the top of the atmosphere is $-22\pm6\,Wm^{-2}$, while at the surface it is $-73\pm12\,Wm^{-2}$, leading to atmospheric forcing of $+51\pm13\,Wm^{-2}$. The global mean clear-sky ARF at the TOA and the surface are found to be negative (Ge et al., 2010; Kim and Ramanathan, 2008; Yu et al., 2006). The TOA and surface forcing for the month of November 2006 range from -14 to $-36\,Wm^{-2}$ with an average value of $-29\pm10\,Wm^{-2}$ and -57 to $-108\,Wm^{-2}$ with an average value of $-88\pm21\,Wm^{-2}$. This results in increasing the atmospheric forcing from $+35$ to $+84\,Wm^{-2}$ with an average value of $+59\pm19\,Wm^{-2}$. Similarly, for July 2007 the forcing is in the range of $+11$ to $-118\,Wm^{-2}$ (average $-35\pm12\,Wm^{-2}$) and -46 to $-130\,Wm^{-2}$ (average $-96\pm33\,Wm^{-2}$) at the TOA and surface, respectively, giving rise to atmospheric forcing from $+42$ to $+85\,Wm^{-2}$ (average $+61\pm21\,Wm^{-2}$). Likewise, the ARF in April 2007 at surface, TOA, and within the atmosphere are in the range of -47 to $-81\,Wm^{-2}$ (average $-62\pm9\,Wm^{-2}$), $+2$ to $-20\,Wm^{-2}$ (average $-7\pm5\,Wm^{-2}$), and $+39$ to $+83\,Wm^{-2}$ (average $+55\pm12\,Wm^{-2}$) respectively. In contrast, the ARF in May is minimum on the surface and within the atmosphere and ranges from -43 to $-68\,Wm^{-2}$ (average $-56\pm9\,Wm^{-2}$), and $+27$ to $+52\,Wm^{-2}$ (average $+41\pm6\,Wm^{-2}$) respectively, but forcing over TOA is relatively higher than in April and is in the range of -7 to$-23\,Wm^{-2}$ (average $-16\pm7\,Wm^{-2}$).

Prasad et al. (2007) reported the surface and TOA forcing in the range of -19 to $-87\,Wm^{-2}$ and $+2$ to $-26\,Wm^{-2}$ respectively during the whole dust period from April–May, 2005, which is comparable to the forcing in the present study
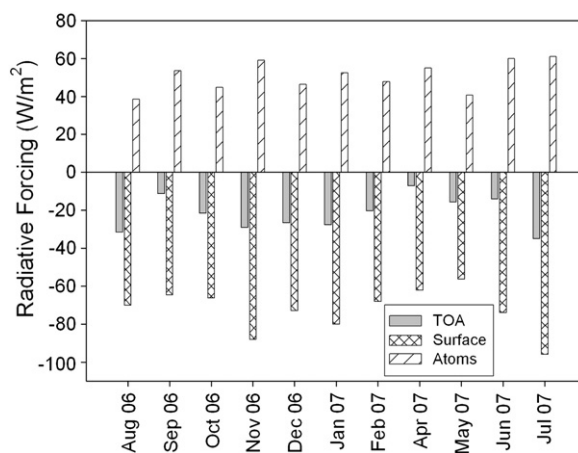

Fig. 8. Monthly averaged variation of simulated aerosol radiative forcing (ARF) over TOA, surface and in the atmosphere for the period August 2006 to July 2007 over Karachi.

for April–May, 2007. Fig. 8 shows that there are large ARF differences between TOA and surface, which demonstrates that solar radiation is absorbed within the atmosphere, consequently heating the atmosphere, reducing eddy heat convergence, and inducing a reduction in surface temperature (Ge et al., 2010; Miller and Tegen, 1999). Furthermore, heating due to absorption of solar radiation by aerosols reaches its maximum close to its uppermost level where the heating is stabilized which in turn may suppress convective activity and prevent cloud formation (Ackerman et al., 2000; Koren et al., 2004). It can be concluded that the presence of ABC over Karachi can considerably decrease the surface and the TOA forcing and enhance the atmospheric forcing.

The ARF values are highest for July 2007 due to the dust storm activities in the southern part of Pakistan. The ARF values are also high for November 2006 due to some dust plumes (Alam et al., 2010) and high black carbon concentrations (Dutkiewicz et al., 2009) over Karachi. The uncertainty in ARF calculation in the present paper may have arisen due to (a) uncertainty in retrieval of AOD (b) uncertainty is SSAs and (c) uncertainty in the surface albedo values. The overall uncertainty in the estimated forcing due to deviations in simulation is found to be 10–15% (Parasad et al., 2007).

Table 3 shows comparisons of radiative forcing at the surface and TOA from AERONET retrievals and SBDART calculations. The forcing at TOA is maximum (maximum negative) for AERONET as compared to SBDART during August 2006–November 2006 and April 2007–July 2007. Likewise, the forcing at the surface is higher (more negative) in August 2006 and July 2007 for AERONET than SBDART, for other months the forcing at surface for AERONET–SBDART is comparable. Overall the TOA forcing is maximum for AERONET than SBDART and the surface forcing is almost similar for AERONET–SBDART except for August 2006 and July 2007. The correlation for the whole period of observation for AERONET–SBDART at the surface and TOA is 0.92 and 0.82, respectively. Overall the comparison shows a convincing agreement for the radiative forcing at the surface and TOA from AERONET and SBDART.

3. Conclusions

The optical properties of aerosol (AOD, Alpha, size distribution, SSA, ASY and RI) have been analyzed over the mega city Karachi between August 2006 and July 2007. High AOD values are found for August 2006, November 2006 and July 2007. The high July AOD values are predominantly caused by dust activities in the southern part of Pakistan, whereas high AOD values for November are due to high black carbon concentrations and to some dust plumes in the vicinity of Karachi. The seasonal variations in aerosol volume size distribution exhibit high variability in the coarse mode, whereas minor variations are observed in the accumulation mode. The volume concentrations in the coarse mode are larger in summer than in other seasons. The SSA and ASY parameters values are wavelength dependent and show high fluctuations throughout the year. The monthly average real parts of RI values are also wavelength dependent and range from 1.41 to 1.57. The monthly average ARF at the TOA varies from -7 to -35 Wm^{-2} throughout the year. The monthly average ARF at the surface and within the atmosphere range from -56 to -96 Wm^{-2} and $+41$ to $+61$ Wm^{-2}, respectively. Direct measurements of dust aerosol size distribution and the chemical/mineralogical composition of dust samples with other instruments such as the Grimm dust spectrometer will be useful in future research to investigate the uncertainties in AERONET size distribution and other optical properties (SSA, ASY, RI). This will lead to more accurate simulations of the radiative forcing calculation. In future research the aerosol optical properties at Karachi will be compared to additional AERONET sites in the region, which will be useful to better understand the regional or local behavior of aerosol optical properties and radiative forcing over the Pakistan region.

Table 3
Comparison of AERONET derived and SBDART calculated radiative forcing at the surface and TOA.

Months	SBDART calculated RF		AERONET derived RF	
	TOA	Surface	TOA	Surface
Aug 2006	-31 ± 7	-70 ± 16	-42 ± 9	-89 ± 24
Sep 2006	-11 ± 6	-65 ± 22	-21 ± 8	-66 ± 19
Oct 2006	-22 ± 8	-66 ± 15	-25 ± 6	-67 ± 21
Nov 2006	-29 ± 11	-88 ± 24	-30 ± 7	-93 ± 39
Dec 2006	-27 ± 13	-73 ± 36	-25 ± 5	-78 ± 21
Jan 2007	-28 ± 8	-80 ± 36	-23 ± 8	-77 ± 20
Feb 2007	-20 ± 5	-68 ± 11	-19 ± 5	-68 ± 15
Apr 2007	-7 ± 5	-62 ± 10	-17 ± 4	-64 ± 12
May 2007	-16 ± 7	-56 ± 9	-20 ± 5	-58 ± 10
Jun 2007	-14 ± 4	-74 ± 22	-20 ± 15	-76 ± 26
Jul 2007	-35 ± 10	-96 ± 32	-39 ± 10	-113 ± 38

References

Ackerman, A.S., Toon, O.B., Stevens, D.E., Heymsfield, A.J., Ramanathan, V., Welton, E.J., 2000. Reduction of tropical cloudiness by soot. Science 288, 1042–1047.

Alam, K., Iqbal, M.J., Blaschke, T., Qureshi, S., Khan, G., 2010. Monitoring spatio-temporal variations in aerosols and aerosol–cloud interactions over Pakistan using MODIS data. Adv. Space Res. 46, 1162–1176.

Arola, A., Schuster, G., Myhre, G., Kazadzis, S., Dey, S., Tripathi, S.N., 2011. Inferring absorbing organic carbon contents from AERONET data. Atmos. Chem. Phys. 11, 215–225.

Badarinath, K.V.S., Madhavi Latha, K., Kiran Chand, T., Prabhat Gupta, K., 2009. Impact of biomass burning on aerosol properties over tropical wet evergreen forests of Arunachal Pradesh. India. Atmos. Res. 91, 87–93.

Behnert, I., Matthias, V., Doerffer, R., 2007. Aerosol climatology from ground-based measurements for the southern North Sea. Atmos. Res. 84, 201–220.

Cheng, T., Wang, H., Xu, Y., Li, H., Tian, L., 2006a. Climatology of aerosol optical properties in northern China. Atmos. Environ. 40, 1495–1509.

Cheng, T., Liu, Y., Lu, D., Xu, Y., Li, H., 2006b. Aerosol properties and radiative forcing in Hunshan Dake desert, northern China. Atmos. Environ. 40, 2169–2179.

Dubovik, O., Smirnov, A., Holben, B.N., King, M.D., Kaufman, Y.J., Eck, T.F., Slutsker, I., 2000. Accuracy assessments of aerosol optical properties retrieved from Aerosol Robotic Network (AERONET) Sun and sky radiance measurements. J. Geophys. Res. 105, 9791–9806.

Dubovik, O., Holben, B.N., Eck, T.F., Smirnov, A., Kaufman, Y.J., King, M.D., Tanre, D., Slutsker, I., 2002. Variability of absorption and optical properties of key aerosol types observed in worldwide locations. J. Atmos. Sci. 59, 590–608.

Dutkiewicz, V.A., Alvi, S., Ghauri, B.M., Choudhary, M.I., Hussain, L., 2009. Black carbon aerosols in urban air in South Asia. Atmos. Environ. 43, 1737–1744.

Ge, J.M., Su, J., Ackerman, T.P., Fu, Q., Huang, J.P., Shi, J.S., 2010. Dust aerosol optical properties retrieval and radiative forcing over northwestern China during the 2008 China–U.S. joint field experiment. J. Geophys. Res. 115 (D00k12). doi:10.1029/2009JD013263.

Haywood, J.M., Francis, P.N., Glew, M.D., Taylor, J.P., 2001. Optical properties and direct radiative effect of Saharan dust: a case study of two Saharan dust outbreaks using aircraft data. J. Geophys. Res. 106, 18417–18430.

Holben, B.N., Eck, T.F., Slutsker, I., Tanré, D., Buis, J.P., Setzer, A., Vermote, E., Reagan, J.A., Kaufman, Y.J., Nakajima, T., Lavenu, F., Jankowiak, I., Smirnov, A., 1998. AERONET—a federated instrument network and data archive for aerosol characterization. Remote. Sens. Environ. 66, 1–16.

Intergovernmental Panel on Climate Change (IPCC), 2001. Climate Change 2001: The Scientific Basis. Cambridge University Press, Cambridge, United Kingdom, New York, NY, USA. 881.

Intergovernmental Panel on Climate Change (IPCC), 2007. Climate change 2007: The physical science basis: Contribution of Working Group I to the Fourth Assessment Report of the Intergovernmental Panel on Climate Change. Chapter 2, pp 129.

Jacobson, M.Z., 2001. Strong radiative heating due to the mixing state of black carbon in atmospheric aerosols. Nature 409, 695–698.

Jayaraman, A., Gadhavi, H., Ganguly, D., Misra, A., Ramachandran, S., Rajesh, T.A., 2006. Spatial variations in aerosol characteristics and regional radiative forcing over India: measurements and modeling of 2004 road campaign experiment. Atmos. Environ. 40, 6504–6515.

Kaskaoustis, D.G., Kambezidis, H.D., Hatzianastassiou, N., Kosmopoulos, P.G., Badarinath, V.S., 2007. Aerosol climatology: on the discrimination of aerosol types over four AERONET sites. Atmos. Chem. Phys. 7, 6357–6411.

Kaufman, Y.J., Tanre, D., Dubovik, O., Karnieli, A., Remer, L.A., 2001. Absorption of sunlight by dust as inferred from satellite and ground-based remote sensing. Geophys. Res. Lett. 28, 1479–1482.

Kim, D.-H., Ramanathan, V., 2008. Solar radiation budget and radiative forcing due to aerosols and clouds. J. Geophys. Res. 113 (D02203). doi:10.1029/2007JD008434.

Koren, I., Kaufman, Y.J., Remer, L.A., Martins, J.V., 2004. Measurement of the effect of Amazon smoke on inhibition of cloud formation. Science 303, 1342–1345.

Kosmopoulos, P.G., Kaskaoutis, D.G., Nastos, P.T., Kambezidis, H.D., 2008. Seasonal variation of columnar aerosol optical properties over Athens, Greece, based on MODIS data. Remote. Sens. Environ. 112, 2354–2366.

Kumar, K.R., Narasimhulu, K., Balakrishnaiah, G., Reddy, S.S., Gopal, K.R., Reddy, R.R., Satheesh, S.K., Moorthy, K.K., Babu, S.S., 2010. A study on the variations of optical and physical properties of aerosols over a tropical semi-arid station during grassland fire. Atmos. Res. 95, 77–87.

Liu, J., Zheng, Y., Li, Z., Wu, R., 2008. Ground-based remote sensing of aerosol optical properties in one city in Northwest China. Atmos. Res. 89, 194–205.

Menon, S., Hansen, J., Nazarenko, L., Luo, Y., 2002. Climate effects of black carbon aerosols in China and India. Science 297, 2250–2253.

Miller, R.L., Tegen, I., 1999. Radiative forcing of a tropical direct circulation by soil dust aerosols. J. Atmos. Sci. 56, 2403–2433.

NASA Earth Observatory Natural Hazards, 2007. Dust storm over Afghanistan and Pakistan. http://earthobservatory.nasa.gov/NaturalHazards/view.php?id=18761.

Otto, S., Reus, M.de., Trautmann, T., Thomas, A., Wendisch, M., Borrmann, S., 2007. Atmospheric radiative effects of an in situ measured Saharan dust plume and the role of large particles. Atmos. Chem. Phys. 7, 4887–4903.

Parekh, P.P., Khwaja, H.A., Khan, A.R., Naqvi, R.R., Malik, A., Shah, S.A., Khan, K., Hussain, G., 2001. Ambient air quality of two metropolitan cities of Pakistan and its health implications. Atmos. Environ. 32, 5971–5978.

Penner, J.E., Zhang, S.Y., Chuang, C.C., 2003. Soot and smoke may not warm climate. J. Geophys. Res. 108 (D21), 4657. doi:10.1029/2003JD003409.

Prasad, A.K., Singh, S., Chauhan, S.S., Srivastava, M.K., Singh, R.P., Singh, R., 2007. Aerosol radiative forcing over the Indo-Gangetic Plains during major dust storms. Atmos. Environ. 41, 6289–6301.

Ramanathan, V., Crutzen, P.J., Lelieveld, J., Mitra, A.P., et al., 2001. Indian ocean experiment: an integrated analysis of the climate forcing and effects of the great Indo-Asian haze. J. Geophys. Res. 106, 28371–28398.

Ramanathan, V., Chung, C., Kim, D., Bettge, T., Buja, L., Kiehl, J.T., Washington, W.M., Fu, Q., Sikka, D.R., Wild, M., 2005. Atmospheric brown clouds: impacts on South Asian climate and hydrological cycle. Proc. Natl. Acad. Sci. U. S. A. 102 (15), 5326–5333.

Ramanathan, V., Agrawal, M., Akimoto, H., Aufhammer, M., Devotta, S., Emberson, L., Hasnain, S.I., Iyngararasan, M., Jayaraman, A., Lawrance, M., Nakajima, T., Oki, T., Rodhe, H., Ruchirawat, M., Tan, S.K., Vincent, J., Wang, J.Y., Yang, D., Zhang, Y.H., Autrup, H., Barregard, L., Bonasoni, P., Brauer, M., Brunekreef, B., Carmichael, G., Chung, C.E., Dahe, J., Feng, Y., Fuzzi, S., Gordon, T., Gosain, A.K., Htun, N., Kim, J., Mourato, S., Naeher, L., Navasumrit, P., Ostro, B., Panwar, T., Rahman, M.R., Ramana, M.V., Rupakheti, M., Settachan, D., Singh, A.K., St. Helen, G., Tan, P.V., Viet, P.H., Yinlong, J., Yoon, S.C., Chang, W.-C., Wang, X., Zelikoff, J., Zhu, A., 2008. Atmospheric brown clouds: Regional assessment report with focus on Asia. United Nations Environment Programme, Nairobi, Kenya.

Ranjan, R.R., Joshi, H.P., Iyer, K.N., 2007. Spectral Variation of Total Column Aerosol Optical Depth over Rajkot: A Tropical Semi-arid Indian Station. AAQR 7, 33–45.

Ricchiazzi, P., Yang, S., Gautier, C., Sowle, D., 1998. SBDART: A research and teaching software tool for plane-parallel radiative transfer in the earth's atmosphere. Bull. Am. Meteorol. Soc. 79, 2101–2114.

Sarkar, S., Chokngamwong, R., Cervone, G., Singh, R.P., Kafatos, M., 2006. Variability of aerosol optical depth and aerosol forcing over India. Adv. Space Res. 37, 2153–2159.

Singh, R.P., Dey, S., Tripathi, S.N., Tare, V., Holben, B.N., 2004. Variability of aerosol parameters over Kanpur city, northern India. J. Geophys. Res. doi:10.1029/2004JD004966.

Singh, S., Soni, K., Bano, T., Tanwar, R.S., Nath, S., Arya, B.C., 2010. Clear-sky direct aerosol radiative forcing variations over mega-city Delhi. Ann. Geophys. 28, 1157–1166.

Smirnov, A., Holben, B.N., Eck, T.F., Dubovik, O., Slutsker, I., 2000. Cloud screening and quality control algorithms for the AERONET data base. Remote. Sens. Environ. 73, 337–349.

Smirnov, A., Holben, B.N., Dubovik, O., Neill, N.T., Eck, T.F., Westphal, D.L., Goroch, A.K., Pietras, C., Slutsker, I., 2001. Atmospheric aerosol optical properties in the Persian Gulf. J. Atmos. Sci. 59, 620–633.

Tegen, I., Werner, M., Harrison, S.P., Kohfeld, K.E., 2004. Relative importance of climate and land use in determining present and future global soil dust emission. Geophys. Res. Lett. 31 (L05105). doi:10.1029/2003GL019216.

Tripathi, S.N., Dey, S., Chandel, A., Srivastava, S., Singh, R.P., Holben, B.N., 2005. Comparison of MODIS and AERONET derived aerosol optical depth over the Ganga Basin. India. Ann. Geophys. 23, 1093–1101.

Xia, X., Wang, P., Chen, H., Gouloub, P., Zhang, W., 2005. Ground-based remote sensing of aerosol optical properties over north China in spring. J. Remote Sens. 9, 429–437.

Yu, X., Cheng, T., Chen, J., Liu, Y., 2006. A comparison of dust properties between China continent and Korea, Japan in East Asia. Atmos. Environ. 40, 5787–5797.

Zheng, Y., Liu, J., Wu, R., Li, Z., Wang, B., Tamio, T., 2008. Seasonal statistical characteristics of aerosol optical properties at a site near dust region in China. J. Geophys. Res. 113, D16205. doi:10.1029/2007JD009384.